Upper-mantle seismic anisotropy from SKS splitting in the South American stable platform: A test of asthenospheric flow models beneath the lithosphere

Marcelo Assumpção[1]*, Marcelo Guarido[1†], Suzan van der Lee[2], and João Carlos Dourado[3]
[1]INSTITUTE OF ASTRONOMY, GEOPHYSICS, AND ATMOSPHERIC SCIENCES, UNIVERSITY OF SÃO PAULO (USP), RUA DO MATÃO 1226, SÃO PAULO, SP 05508-090, BRAZIL
[2]DEPARTMENT OF EARTH AND PLANETARY SCIENCES, NORTHWESTERN UNIVERSITY, 1850 CAMPUS DR., EVANSTON, ILLINOIS 60208-2150, USA
[3]INSTITUTE OF GEOSCIENCES (IGCE), STATE UNIVERSITY OF SÃO PAULO (UNESP), AV. 24-A 1515, RIO CLARO, SP 13506-900, BRAZIL

ABSTRACT

Upper-mantle seismic anisotropy has been extensively used to infer both present and past deformation processes at lithospheric and asthenospheric depths. Analysis of shear-wave splitting (mainly from core-refracted SKS phases) provides information regarding upper-mantle anisotropy. We present average measurements of fast-polarization directions at 21 new sites in poorly sampled regions of intraplate South America, such as northern and northeastern Brazil. Despite sparse data coverage for the South American stable platform, consistent orientations are observed over hundreds of kilometers. Over most of the continent, the fast-polarization direction tends to be close to the absolute plate motion direction given by the hotspot reference model HS3-NUVEL-1A. A previous global comparison of the SKS fast-polarization directions with flow models of the upper mantle showed relatively poor correlation on the continents, which was interpreted as evidence for a large contribution of "frozen" anisotropy in the lithosphere. For the South American plate, our data indicate that one of the reasons for the poor correlation may have been the relatively coarse model of lithospheric thicknesses. We suggest that improved models of upper-mantle flow that are based on more detailed lithospheric thicknesses in South America may help to explain most of the observed anisotropy patterns.

LITHOSPHERE; v. 3; no. 2; p. 173–180. doi: 10.1130/L99.1

INTRODUCTION

Seismic anisotropy in upper-mantle rocks is due mainly to the lattice preferred orientation (LPO) of olivine (e.g., Nicolas and Christensen, 1987), the most abundant and deformable mineral in the upper mantle. Because LPO depends on the strain history, the study of seismic anisotropy has been extensively used to obtain information on the strain-induced fabric within Earth's interior. Anisotropy in the upper mantle may result from both past and current deformation. Past orogenic processes can imprint the lithospheric upper mantle with a crystallographic fabric that can remain stable after thermal relaxation, which is often called "frozen anisotropy" (e.g., Nicolas and Christensen, 1987; Vauchez and Nicolas, 1991; Ben Ismaïl and Mainprice, 1998; Savage, 1999; Fouch and Rondenay, 2006; Plomerová et al., 2008). Current deformation and flow of the asthenospheric mantle, which is related to plate motion, also causes olivine LPO. This is the main cause of upper-mantle anisotropy beneath oceanic basins (e.g., Tommasi, 1998; Wolfe and Silver, 1998; Conrad et al., 2007).

*E-mail: marcelo@iag.usp.br.
†Current Address: WesternGeco, Houston, TX, USA

A shear wave propagating through an anisotropic medium is split into two shear waves (a fast and a slow component) polarized in mutually perpendicular directions. Thus, polarization analysis of SKS phases (a nearly vertical propagating S wave converted from a P wave at the core-mantle boundary) yields information mainly on the upper-mantle anisotropy beneath the receiving seismic station. Anisotropy can also be observed in the crust, both from the preferred orientation of cracks (e.g., Crampin, 1985) and from the metamorphic grain (Barruol and Mainprice, 1993), in the transition zone and lower mantle, (e.g., Trampert and van Heijst, 2002; Tommasi et al., 2004; Wookey et al., 2002) and in the D″ layer (Kendall and Silver, 1998). Although anisotropy measured with SKS phases represents the vertically integrated effect of anisotropy from the core-mantle boundary to the surface, seismological and petrophysical studies (e.g., Silver, 1996; Savage, 1999; Gung et al., 2003) indicate that the main source of anisotropy that causes splitting of teleseismic SKS waves is located within the first 400 km of the upper mantle.

SKS splitting is easily measured, and there are now large data sets for most continents from which inferences about upper-mantle deformation processes can be made. Along orogenic belts, such as the Andean chain, complex anisotropy patterns can arise, and strong influence from the asthenospheric wedge is common; an example is the trench-parallel flow first observed by Russo and Silver (1994). However, even in midplate continental areas, the main cause of the anisotropy that produces SKS splitting is still controversial (e.g., Savage, 1999; Fouch and Rondenay, 2006). In stable continental areas, Vinnik et al. (1992) attributed most of the observed anisotropy to flow in the asthenosphere due to absolute plate motion. On the other hand, Silver and Chan (1991) and Silver (1996) argued that the measured fast-polarization directions correlated better with the orientation of the tectonic structures resulting from past or ongoing deformation of the lithosphere than with absolute plate motion (e.g., Barruol et al., 1997a). Savage (1999) and Fouch and Rondenay (2006) reviewed the debate regarding the dominant cause of anisotropy in stable continental areas, that is, lithospheric (frozen) versus asthenospheric (current upper mantle flow). They recognized that no single hypothesis can easily explain all of the observations and that both lithospheric and asthenospheric anisotropies contribute to the observed shear-wave

splitting beneath continents, with asthenospheric flow perhaps being channeled around deep lithospheric keels (e.g., Bormann et al., 1996; Barruol et al., 1997b; Fouch et al., 2000; Assumpção et al., 2006).

Despite this long-lasting debate, interpretation of the main origin of upper-mantle anisotropy that causes SKS splitting is far from resolved. For example, Vecsey et al. (2007) and Eken et al. (2010) showed that strong regional variations of the splitting parameter in Fennoscandia can only be explained by predominantly frozen anisotropy in the Precambrian mantle lithosphere. On the other hand, Wang et al. (2008) also used short-scale changes in SKS splitting parameters across the Colorado Plateau and the Great Basin as evidence of a transition from flow due to absolute plate motion beneath the Colorado Plateau to edge-driven small-scale flow around a cratonic keel.

Few seismic anisotropy measurements have been made in South America east of the Andes, and lithospheric, as well as asthenospheric, sources have been invoked as causes of SKS splitting. James and Assumpção (1996) showed that the fast-polarization direction in SE Brazil varies according to structural trends and favored frozen anisotropy in the lithosphere as the main mechanism causing SKS splitting. On the other hand, data from a few stations in southern South America (Helffrich et al., 2002) have revealed fast-polarization directions parallel to the present absolute plate motion. Detailed analysis of SKS splitting in the transcurrent Ribeira fold belt (SE Brazilian coast) by Heintz et al. (2003) suggested contributions from both lithospheric and asthenospheric sources. More recent analysis of a larger data set in SE and central Brazil (Assumpção et al., 2006) indicated that most fast-polarization directions are roughly parallel to the absolute plate motion (in the hotspot reference frame) and that deviations from this absolute plate motion could be attributed to mantle flow around a cratonic keel.

Conrad et al. (2007) compared a global data set of SKS splitting with numerical models of upper-mantle flow. SKS data for oceanic basins showed good correlation with upper-mantle flow, confirming the predominance of asthenospheric sources for oceanic anisotropy. However, for the continents, the generally poor correlation was interpreted as indicating a strong influence of frozen anisotropy in the continental lithosphere. Here, we present new average measurements of SKS splitting from 21 additional stations (Fig. 1), many of them from the Brazilian Lithosphere Seismic Project 2002 (BLSP02; Feng et al., 2004; Lloyd et al., 2010). This new data set, which is especially focused on northern Brazil, will contribute to the comparison between observations and theoretical models.

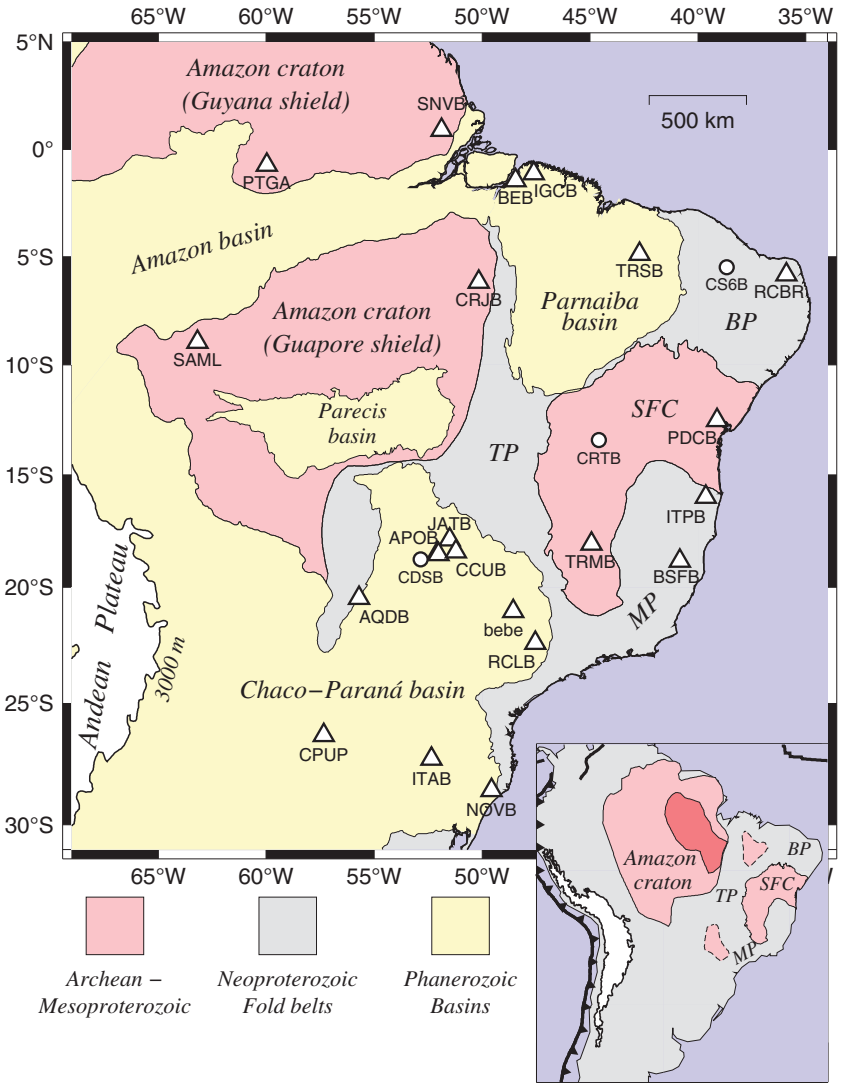

Figure 1. Stations with new measurements of SK(K)S splitting in South America (shown as triangles; see Table 1). Circles are stations with no clearly defined SKS splitting. Colors show the main geological provinces in the stable part of South America (Schobbenhaus and Bellizzia, 2000). SFC—São Francisco craton. The geological provinces composed mainly of Neoproterozoic (Brasiliano) fold belts are: Tocantins (TP), Borborema (BP), and Mantiqueira (MP). The inset shows the major cratons and the inferred cratonic blocks beneath the Paraná and Parnaíba Basins; the darker pink in the Amazon craton is the oldest Archean nucleus (Tassinari and Macambira, 1999).

The stable South American platform is composed of two major Archean to Mesoproterozoic cratons (Fig. 1): the Amazon craton, exposed in the Guyana and Guaporé Shields, and the São Francisco craton. Early Archean units are found in the northeastern part of the Amazon craton (Central Amazonian Province, older than 2.3 Ga; Tassinari and Macambira, 1999; Fig. 1, inset) and the middle part of the São Francisco craton (Alkmim et al., 2001). Surface-wave tomography by Feng et al. (2004, 2007) showed that the highest S-wave velocity anomalies in the depth range of 150–250 km occur in these two older provinces; such anomalies indicate areas with the thickest lithosphere. Older (Proterozoic) cratonic fragments have been inferred to be buried beneath the Parnaíba and Paraná Basins (e.g., Cordani et al., 1984; Julià et al., 2008; as shown in Fig. 1, inset). Surface-wave tomography (Feng et al., 2007) and body-wave tomography (Schimmel et al., 2003; Rocha et al., 2010) show generally high velocities beneath these two large basins, which is consistent with these old cratonic basements.

The final amalgamation of all of these large and small cratonic blocks, which formed part of the Gondwana supercontinent in Neoproterozoic–early Paleozoic times (Brasiliano orogen), occurred through several fold belts distributed in three tectonic provinces of the Brasiliano orogen: Tocantins (between the Amazon and São Francisco cratons), Mantiqueira (along the SE coast), and Borborema in NE Brazil (Fig. 1). Soon after the assemblage of Gondwana, four major intracratonic basins started to form in the early Paleozoic: the Solimões-Amazon, Parecis, Parnaíba, and Chaco-Paraná Basins.

MEASUREMENTS OF SKS SPLITTING

Two shear-wave splitting parameters were measured at each station assuming a predominantly horizontal orientation of the fast symmetry axis: (1) φ, the polarization direction of the fast S wave, which is regarded as a reliable proxy for the orientation of the [100] axis of olivine in the upper mantle; and (2) *dt*, the delay between the arrival times of the fast and slow split waves. The value of *dt* is proportional to the intrinsic anisotropy and thickness of the anisotropic layer. These two parameters were calculated with Silver and Chan's (1991) algorithm: The fast polarization direction (φ) and the lag time (*dt*) were determined through a grid search by correcting the observed components from the anisotropy effect to minimize the energy on the corrected transverse component. Examples are shown in Figures 2 and 3 for stations IGCB and BEB near the northern coast. Most of the analyses were made using the program Splitlab (Wüstefeld et al., 2008), a script for Matlab™. The influences of filtering and time windowing were checked, and only robust data showing no significant variations with respect to small changes in the window size were considered reliable.

Earthquakes with magnitude larger than 5.5 m_b and in the distance range of between 90° and 130° were analyzed for SKS and SKKS phases; the distance range 130°–165° was also used for SKKS phases. Individual results were classified as "good" or "fair." "Good" results exhibit small errors (<15° and ≤0.4 s for φ and *dt*, respectively), show good signal-to-noise ratios in the transverse components, show elliptical particle motion in the horizontal components before correction and linear motion after anisotropy removal, and have good waveform coherency between the fast and slow shear waves. Results satisfying three of the four criteria were classified as "fair," and those satisfying only two or less were discarded, as was done by Heintz et al. (2003) and Assumpção et al. (2006). The examples shown in Figures 2 and 3 are "good" measurements: φ = −58° ± 5°, *dt* = 0.7 ± 0.2 s (IGCB) and φ = −50° ± 8°, *dt* = 1.3 ± 0.4 s (BEB).

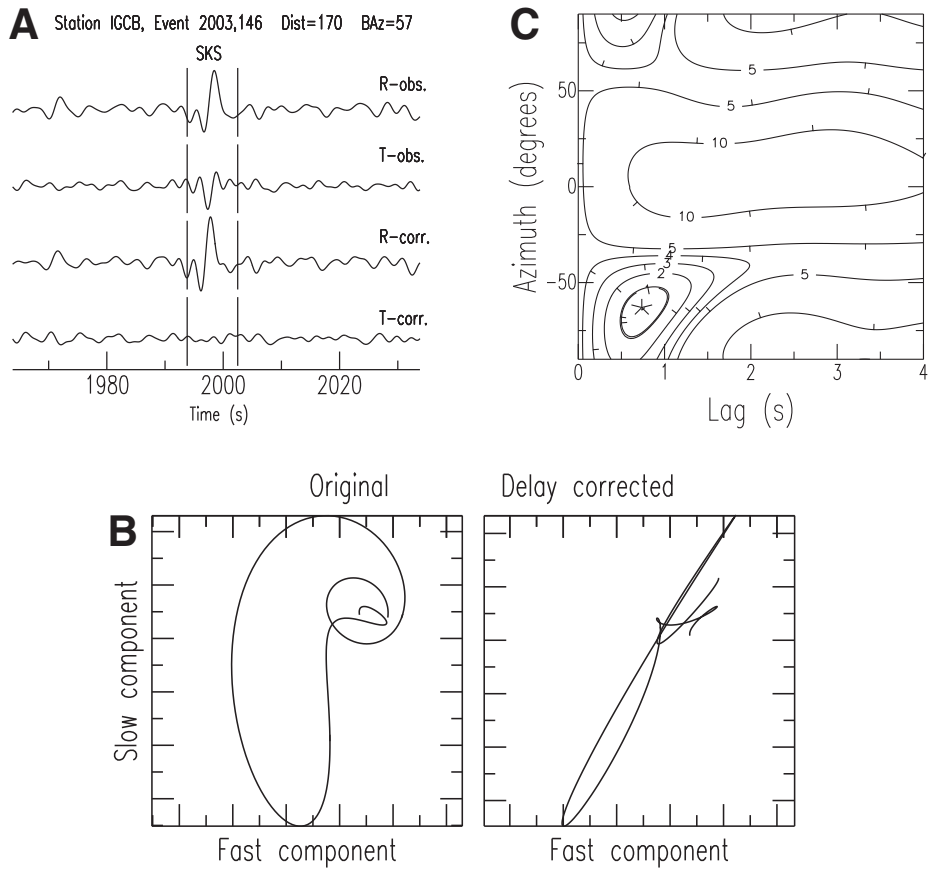

Figure 2. Example of a splitting determination for a SKKS phase at the IGCB station (Igarapé Açu, Pará, northern Brazil). (A) Original and corrected radial and transverse components. (B) Original particle motion, particle motion after removal of the anisotropy effect. (C) Contour lines of the transverse energy for corrections by various delays ("lag") and fast-polarization directions ("azimuth"). This measurement is ranked as "good quality" with ϕ = –58° (±5°) and *dt* = 0.7 s (±0.2 s).

When the wave has an initial polarization that is parallel or orthogonal to the fast- or slow-polarization direction, or if there is no anisotropy beneath the station, no splitting will occur, and no energy will be observed on the transversal component. Such a measurement is known as "null" and would be expected along the "null lines" in Figure 4. For the stations shown in Figure 4, no clear null was observed (a null measurement usually requires data with very high signal-to-noise ratios).

Here, we assume anisotropy to be located predominantly in a single layer with horizontal symmetry axes. Figure 4 shows our measurements at six stations in northern Brazil as a function of the event back azimuth. Stations CRJB, IGCB, PTGA, and SNVB show consistent fast directions (to within ±15°) from different back azimuths. As a first approximation, these stations are then consistent with the hypothesis of single values of ϕ and *dt*. More complex anisotropy geometries (double anisotropic layers or dipping axes of symmetry) are not ruled out but require many more observations from different back azimuths and cannot be considered here.

We classified the average value for each station as either A or B quality. A station ranked as "A" quality has four or more consistent measurements with a 95% confidence limit in the mean fast-polarization direction smaller than 10°. Uncertainties between 10° and 25° or with less than four measurements were considered "B" quality. Confidence limits larger than 25° may indicate weak anisotropy or more complex anisotropic geometries and were not included in our analysis.

For the permanent station PTGA, we measured 13 SK(K)S phases, which gave average values of ϕ = 87° ± 7° and *dt* = 1.1 ± 0.3 s. Krüger et al. (2002) analyzed 20 phases giving

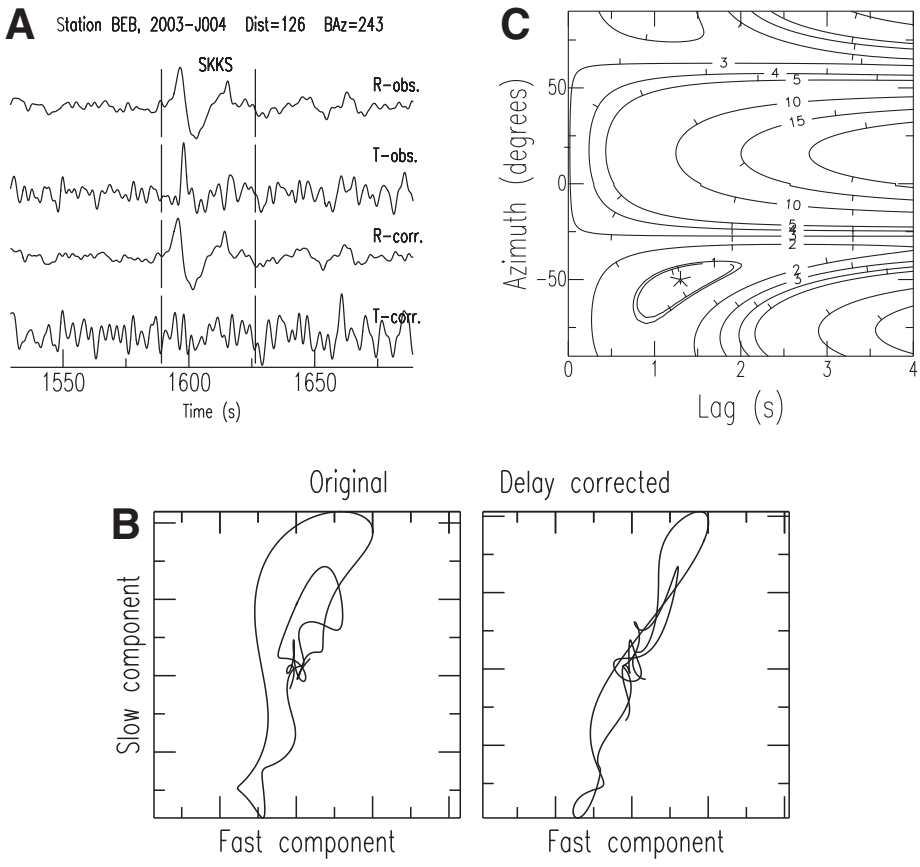

Figure 3. Example of a splitting determination for a SKKS phase at the BEB station (Belém, PA, northern Brazil). (A) Original and corrected radial and transverse components (traces not to scale). (B) Original particle motion and particle motion after removal of the anisotropy effect. (C) Contour lines of the transverse energy for corrections by various delays ("lag") and fast-polarization directions ("azimuth"). This measurement is ranked as "good quality" with $\phi = -50°$ (±8°) and $dt = 1.3$ s (±0.4 s).

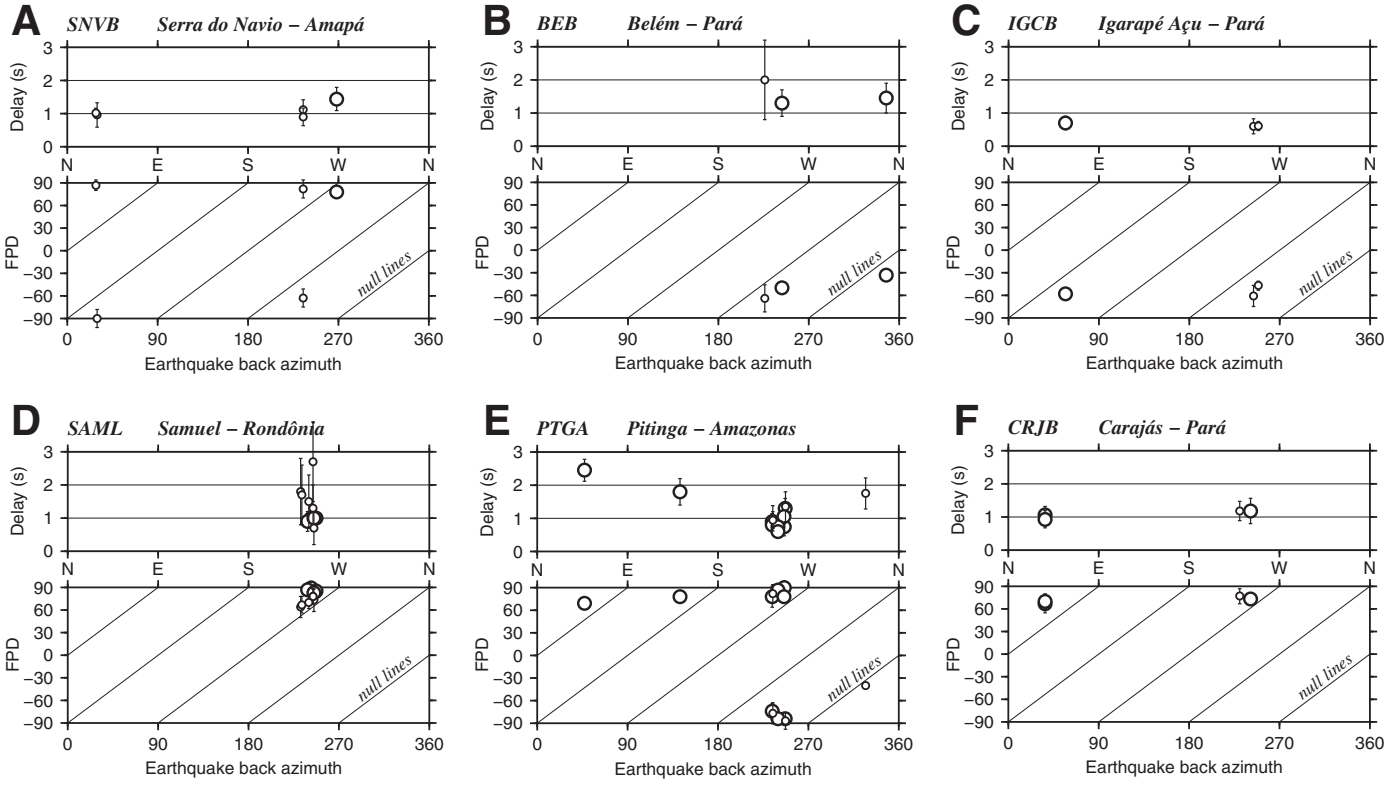

Figure 4. Splitting results from the stations SNVB, BEB, IGCB, SAML, PTGA, and CRJB in northern Brazil, plotted with respect to the back azimuths of the events. The time delay is in the top diagram, and the fast polarization direction (FPD) is in the bottom diagram. The lines on the FPD plots represent the expected loci for null results.

different average directions at 110° ± 10°. Most events with good signal-to-noise ratios have a SW back azimuth. For these SW events, our measurements give a systematic difference of 17° with respect to Krueger et al.'s values but are consistent with the average direction of 101° ± 10° that was determined by Ivan et al. (2001).

Table 1 shows the average results for the 21 new stations analyzed here, and Figure 5 compares all available results for the stable part of South America (from this work and previously published papers; see Fig. 5 legend), with the S-wave velocity anomalies from the surface-wave tomography of Feng et al. (2007). Qualities A and B are indicated by the thicknesses of the bars in Figure 5.

RESULTS AND DISCUSSION

Pattern of Station Averages

A compilation of previous fast directions in South America, together with our new data (Table 1), is presented in Figure 5. In the Andes (despite a somewhat large scatter), a trend of coast-parallel fast directions can be seen, as was first recognized by Russo and Silver (1994). This trend is attributed mainly to trench-parallel asthenospheric flow beneath the subduction zone. In some areas, a complex pattern can arise from small-scale convection in the asthenospheric wedge, as well as from contributions from both the South American and the subducted Nazca lithospheres (Polet et al., 2000; Anderson et al., 2004). Near the Caribbean border, the influence of E-W transcurrent motion at the plate border can be seen in the data of Piñero-Feliciangeli and Kendall (2008) and Growdon et al. (2009).

In the stable part of South America (east of the Andean front), a more uniform pattern can be recognized, where most fast directions are oriented E-W or ENE-WSW and roughly parallel to the absolute plate motion in the hotspot reference frame (HS3-NUVEL-1A model by Gripp and Gordon, 2002). This can be seen in the histogram in Figure 6. Most of the large deviations from this absolute motion arise from the NW-SE directions at the southern part of the São Francisco craton, around the high S-wave velocity anomaly (Fig. 5). This was described by Assumpção et al. (2006) as being mainly attributable to asthenospheric flow around the southern keel of the São Francisco craton.

The positive and negative S-wave anomalies derived from the surface-wave tomography (Feng et al., 2007) are only a qualitative indication of areas with a thicker or thinner lithosphere, respectively, because no "direct" measurements (i.e., using seismic-converted phases) of lithospheric thickness have been made. However, direct estimates of the lithosphere-asthenosphere boundary using S-wave receiver functions (Heit et al., 2007) are remarkably consistent with the S-wave anomalies seen in Figure 5. Because of the large number of sizable earthquakes necessary to obtain a good stacked S-wave receiver-function, a reliable lithosphere-asthenosphere boundary signal is only available in South America for some permanent stations with many years of operation. The thickest lithosphere (160 km) was found beneath station BDFB in central Brazil, where S-wave anomalies are about +3% at 150 km depth (Fig. 5). A very thin continental lithosphere (less than 100 km) is generally found to be associated with negative S-wave anomalies of −3%, such as beneath stations CPUP and TRQA, or very close to the coast (e.g., RCBR in NE Brazil and MPG in French Guyana). Station SAML in the Amazon craton shows an intermediate lithospheric thickness (130 km) corresponding to very small velocity anomalies. In the Paraná Basin, a stack of about 10 temporary stations shows an average lithosphere-asthenosphere boundary of 120 km depth, which is also consistent with the average S-wave anomalies less than 2% in that area (Fig. 5).

The generally good correlation of lithosphere-asthenosphere boundary depths and S-wave anomalies implies that the tomography results do indicate two separate cratonic keels, one in the eastern part of the Amazon craton, and the other in the southern part of the São Francisco craton. Despite the few anisotropy measurements available for the Amazon region, the fast-polarization directions seem to suggest flow roughly parallel to the absolute plate motion (APM) to the east of the Amazonian keel (defined by the large positive S-wave anomaly centered at 4°S, 52°W) and a possible closing of the flow just behind the keel (at stations BEB and IGCB). This suggests a deviation of upper-mantle flow around the keel of the Amazon craton, as was similarly observed around the São Francisco keel in southeastern Brazil (Assumpção et al., 2006). In addition, the WNW-ESE orientation of the fast directions observed in the southern part of the Chaco-Paraná Basin (near latitudes 26°–27°S and beneath stations CPUP and ITAB) could perhaps be attributed to asthenospheric flow in a low-velocity channel beneath a thin lithosphere.

Table 1. New SKS splitting results for the stable part of South America

Station	Latitude (°S)	Longitude (°W)	φ (°)	dφ (°)	δt (s)	dδt (s)	N
APOB	18.5471	52.0251	83	8	1.9	0.4	4
APOB2	18.5081	52.0740	102	13	1.3	0.2	9
AQDB*	20.4760	55.6990	90	15	0.9	0.2	4
BEB*	1.4503	48.4443	137	12	1.4	0.3	3
bebe	21.0400	48.5500	72	9	0.9	0.2	8
BSFB	18.8313	40.8465	73	6	1.6	0.3	6
CCUB	18.4250	51.2120	70	10	2.0	1.0	2
CPUP	26.3306	57.3309	104	10	1.2	0.1	11
CRJB*	6.1702	50.1546	71	4	1.1	0.1	4
IGCB*	1.1272	47.6085	124	6	0.6	0.1	3
ITAB*	27.3082	52.3411	104	4	1.3	0.2	6
ITPB*	15.9887	39.6282	99	2	1.4	0.2	1
NOVB*	28.6105	49.5582	82	5	1.6	0.2	2
PDCB*	12.5306	39.1238	33	11	1.0	0.3	4
PTGA	0.7308	59.9666	87	10	1.1	0.3	13
RCBR	5.8275	35.9014	9	11	1.9	0.2	9
RCLB	22.4191	47.5310	85	9	0.9	0.2	14
SAML	8.9488	63.1832	76	9	1.0	0.3	11
SNVB*	0.9051°N	51.8771	84	10	1.1	0.2	5
TRQA	38.0567	61.9795	134	10	1.2	0.1	16
TRSB*	4.8730	42.7059	105	20	0.8	0.3	9

Note: φ—fast polarization direction; δ*t*—splitting delay time; *d*φ and *d*δ*t*—uncertainties (95% confidence limit); *N*—number of measurements. Station "bebe" is the average measurement for two nearby stations that are less than 5 km apart.
*Stations were deployed by the BLSP02 project.

Comparison with Flow Model

Conrad et al. (2007) compared measured fast-polarization directions (from a global compilation of SKS analyses) with upper-mantle flow directions derived from convection models. While the correlation was very good for ocean-island stations (indicating a predominance of asthenospheric flow beneath the lithosphere-asthenosphere boundary as the main cause of SKS splitting in oceanic plates), it was much weaker for continental areas. Conrad et al.

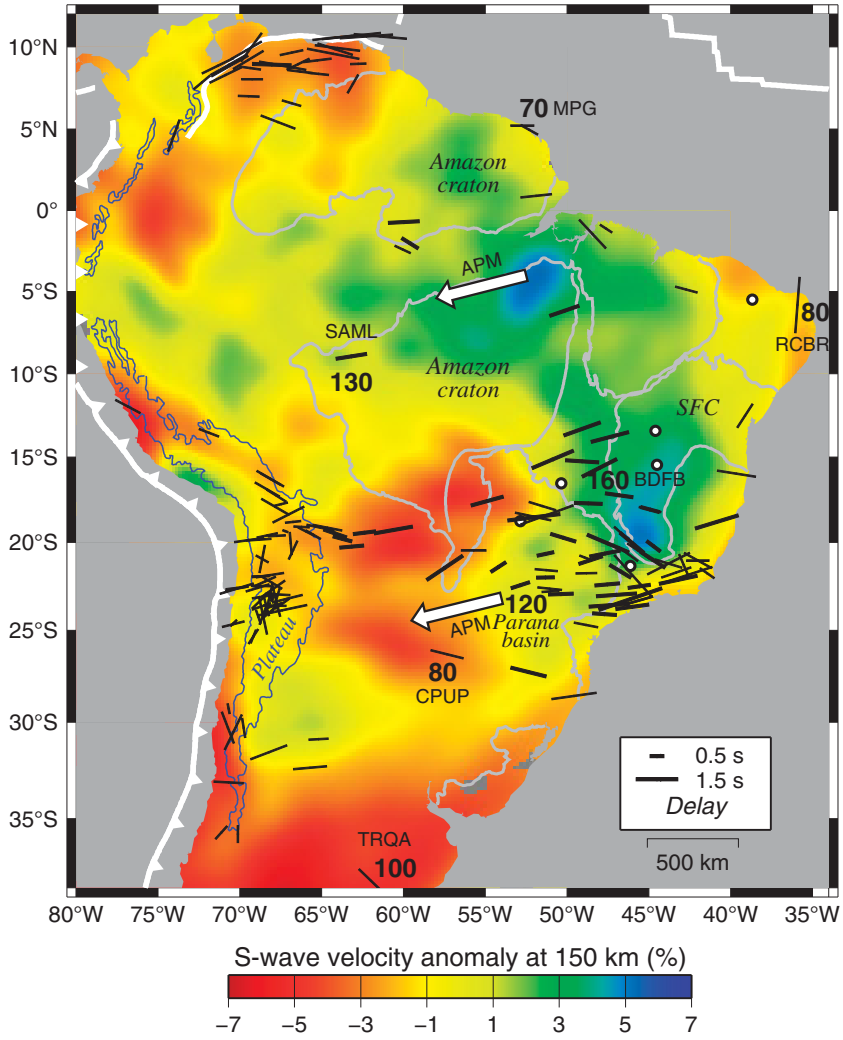

Figure 5. SK(K)S fast directions from this paper (Table 1; stations in Fig. 1) and other published results (Russo and Silver, 1994; James and Assumpção, 1996; Polet et al., 2000; Krüger et al., 2002; Heintz et al., 2003; Anderson et al., 2004; Assumpção et al., 2006; Piñero-Feliciangeli and Kendall, 2008; Growdon et al., 2009; Masy et al., 2009). The bar lengths indicate delay times; bar thicknesses denote the qualities of the stations' average results as in Table 1. Open circles are stations with no reliable SKS measurements. Colors indicate S-wave velocity anomalies at 150 km depth from the surface-wave tomography of Feng et al. (2007). Numbers are depths to the lithosphere-asthenosphere boundary from the S-wave receiver functions (Heit et al., 2007) and are identified by station names. The open arrows indicate the absolute motion of the South American plate in the hotspot reference frame HS3-NUVEL-1A (Gripp and Gordon, 2002). Thick white lines are plate boundaries; the thin blue line is the Andean plateau defined at 3000 m altitude. SFC—São Francisco craton.

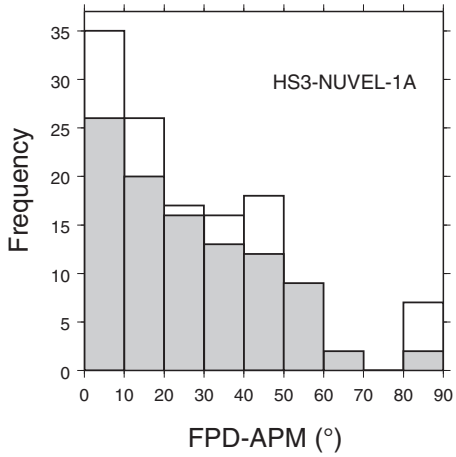

Figure 6. Comparison of all station-average fast-polarization directions (FPD) with the absolute plate motion (APM) given by the HS3-NUVEL-1A model (Gripp and Gordon, 2002). Gray columns are measurements from within the stable platform (i.e., all of the continent except for the Andean belt), and white columns include stations in the Andean belt.

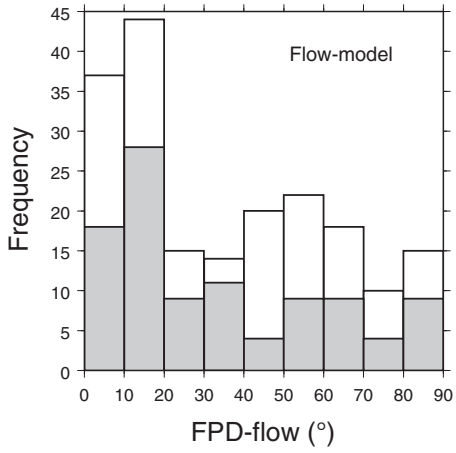

Figure 7. Misfit between all station-average fast-polarization directions (FPD) and the directions of the upper-mantle flow calculated using the model of Conrad et al. (2007). Gray columns are measurements from within the stable platform (i.e., all of the continent except for the Andean belt), and white columns include stations in the Andean belt.

(2007) interpreted this result as evidence for a significant contribution from frozen anisotropy within the continental lithosphere. The convection pattern was driven by density contrasts estimated from seismic velocity anomalies using the global tomographic model S20RTSb of Ritsema et al. (2004). The convection model used the lithospheric thicknesses of the rigid plates derived from seismic velocities (such as used by Gung et al., 2003; Conrad and Lithgow-Bertelloni, 2006). As an example of the relatively poor correlations for the continents, Figure 7 compares all SKS fast-polarization directions in the stable part of South America with the expected flow directions obtained from Conrad et al.'s (2007) preferred numerical model of upper-mantle convection.

Figure 8 shows the flow directions at 225 km depth (black bars) given by the convection model of Conrad et al. (2007). This depth shows the best correlation with the fast polarization directions for the continents on a global scale (Conrad et al., 2007). Figure 8 also shows the 200 km contour (dashed blue line) for lithosphere thickness in midplate South America, which corresponds to a +2% velocity anomaly in the S20RTSb model as used by Gung et al. (2003) and by Conrad and Lithgow-Bertelloni (2006). One can see that the calculated flow direction is diverted by the thick lithosphere in

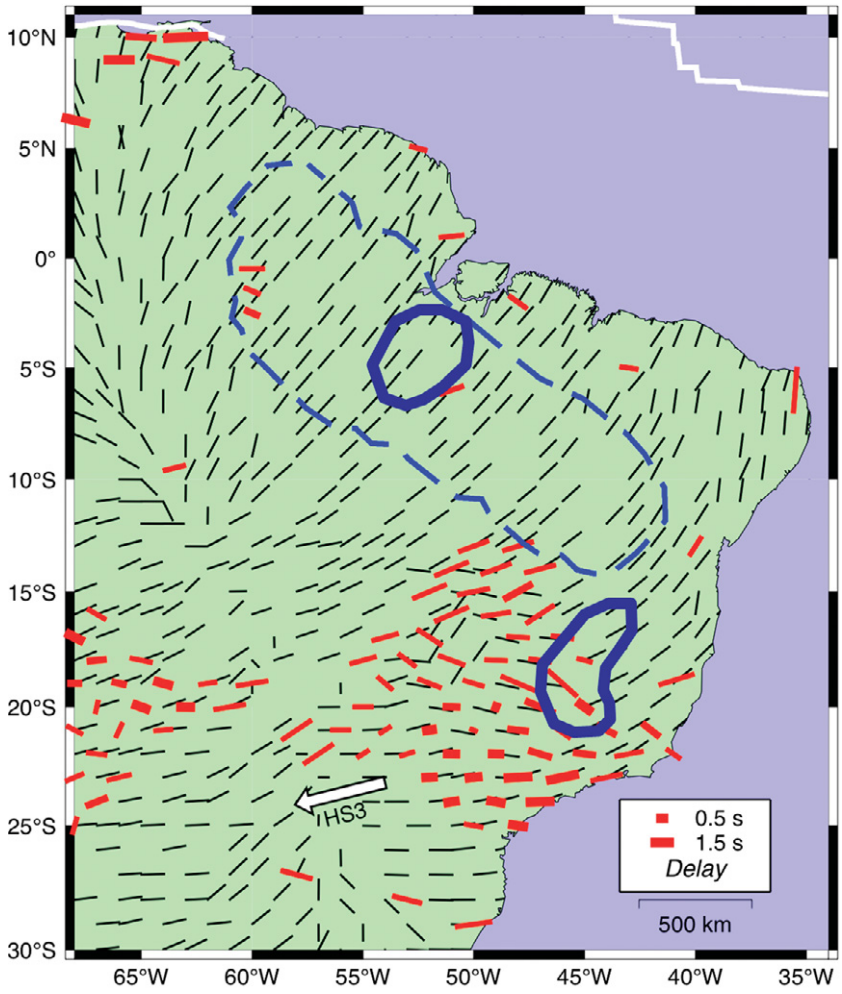

Figure 8. Upper-mantle flow directions (black bars) beneath South America at 225 km depth (model of Conrad et al., 2007) compared with the observed fast-polarization directions averaged at 1° grid spacing (red bars). Thicker bars indicate more reliable mean directions. The white arrow is the absolute plate motion (HS3-NUVEL-1A). The dashed blue line indicates the 200-km-thick lithosphere, corresponding to a +2% velocity anomaly in the global tomography model of Ritsema et al. (2004) as used by Conrad et al. (2007) to derive the convection model. The continuous blue lines are the +4% S-velocity anomaly at 150 km depth from Feng et al. (2007) and indicate the two separate cratonic keels, one in the eastern part of the Amazon craton and the other in the São Francisco craton.

northern Brazil. Figure 8 also shows the two separate cratonic keels (solid blue lines) corresponding to a +4% velocity anomaly at 150 km in Feng et al.'s (2007) regional tomography model. The observed SKS fast directions are shown as red bars calculated by averaging station values around grid points spaced 1° apart.

We believe that the poor correlation between the observed fast-polarization directions and the numerically calculated upper-mantle flow in South America (Fig. 7) may be due to the poor resolution of the lithospheric thickness used in Conrad's global model. For example, in central Brazil (near 15°S, 50°W in Fig. 8), the large discrepancies between the observed SKS fast-polarization directions and the flow directions are probably caused by the deviation of the calculated flow around the southern limit of the S20RTSb cratonic keel (near 10°S). The more detailed tomography model of Feng et al. (2007) shows that the flow deviation should actually occur much further south, around the deep keel of the São Francisco craton near 20°S.

CONCLUSIONS

Here, we present new measurements of SKS splitting for the Amazon region of northern Brazil, a large, previously unsampled area of the South American stable platform. In continental midplate South America, the fast-polarization directions are relatively uniform and show better correlation with the absolute plate motion (HS3-NUVEL-1A reference frame) than with asthenospheric flow directions estimated from large-scale models of upper-mantle convection (Conrad et al., 2007). However, the few measurements in the Amazon region are consistent with the hypothesis that the upper-mantle flow is being diverted by a small but thick lithospheric keel in the Amazon craton (as mapped by the surface-wave tomography of Feng et al., 2007). We propose that the poor correlation between the observed SKS fast directions and the expected asthenospheric LPO (as estimated by flow models of the upper mantle) may not necessarily imply the predominance of frozen anisotropy in the South American lithosphere. Instead, this poor correlation may be due to the poor resolution of the lithospheric thicknesses used to derive the global-scale upper-mantle convection model.

ACKNOWLEDGMENTS

This work was carried out with support from CNPq (Brazilian National Research Council) scholarship 308861/2006-0 and FAPESP (São Paulo State Research Foundation) grants 01/06066-6, 02/00244-2, and 05/51035-2. ETH-Z (Federal Institute of Technology, Zürich, Switzerland), Switzerland (grant 0-20990-02), provided financial support and seismic equipment for the BLSP02 field deployment. We thank Federica Marone, Mark Van der Meijde, Eduardo Mandel, and José Roberto Barbosa for installation and maintenance of the BLSP02 stations. We thank an anonymous reviewer for the detailed analysis of the first version and the many suggestions to improve the paper.

REFERENCES CITED

Alkmim, F.F., Marshak, S., and Fonseca, M.A., 2001, Assembling West Gondwana in the Neoproterozoic: Clues from the São Francisco craton region, Brazil: Geology, v. 29, p. 319–322, doi:10.1130/0091-7613(2001)029<0319:AWGITN>2.0.CO;2.

Anderson, M.L., Zandt, G., Triep, E., Fouch, M., and Beck, S., 2004, Anisotropy and mantle flow in the Chile-Argentina subduction zone from shear wave splitting analysis: Geophysical Research Letters, v. 31, L23608, doi:10.1029/2004GL020906.

Assumpção, M., Heintz, M., Vauchez, A., and Egydio-Silva, M., 2006, Upper mantle anisotropy in SE and central Brazil from SKS splitting: Evidence of asthenospheric flow around a cratonic keel: Earth and Planetary Science Letters, v. 250, p. 224–240, doi:10.1016/j.epsl.2006.07.038.

Barruol, G., and Mainprice, D., 1993, A quantitative evaluation of crustal rocks to the shear-wave splitting of teleseismic SKS waves: Physics of the Earth and Planetary Interiors, v. 78, no. 3–4, p. 281–300, doi:10.1016/0031-9201(93)90161-2.

Barruol, G., Helffrich, G., Russo, R., and Vauchez, A., 1997a, Shear wave splitting around the northern Atlantic: Frozen Pangean lithospheric anisotropy?: Tectonophysics, v. 279, p. 135–148, doi:10.1016/S0040-1951(97)00126-1.

Barruol, G., Silver, P.G., and Vauchez, A., 1997b, Seismic anisotropy in the eastern United States: Deep structure of a complex continental plate: Journal of Geophysical Research, v. 102, no. B4, p. 8329–8348, doi:10.1029/96JB03800.

Ben Ismaïl, W., and Mainprice, D., 1998, An olivine fabric database: An overview of upper mantle fabrics and seismic anisotropy: Tectonophysics, v. 296, p. 145–157, doi:10.1016/S0040-1951(98)00141-3.

Bormann, P., Grunthal, G., Kind, R., and Montag, H., 1996, Upper mantle anisotropy beneath central Europe from SKS wave splitting: Effects of absolute plate motion and lithosphere-asthenosphere boundary topography: Journal of Geodynamics, v. 22, p. 11–32, doi:10.1016/0264-3707(96)00014-2.

Conrad, C.P., and Lithgow-Bertelloni, C., 2006, Influence of continental roots and asthenosphere on plate-mantle coupling: Geophysical Research Letters, v. 33, L05312, doi:10.1029/2005GL025621.

Conrad, C.P., Behn, M.D., and Silver, P.G., 2007, Global mantle flow and the development of seismic anisotropy: Differences between the oceanic and the continental upper mantle: Journal of Geophysical Research, v. 112, B07317, doi:10.1029/2006JB004608.

Cordani, U.G., Brito Neves, B.B., Fuck, R.A., Porto, R., Thomas Filho, A., and Cunha, F.M.B., 1984, Estudo preliminar de integração do pré-Cambriano com os eventos tectônicos das bacias sedimentares brasileiras: Rio de Janeiro, Brazil, Série Ciência-Técnica-Petróleo, v. 15, 70 p., PETROBRAS.

Crampin, S., 1985, Evaluation of anisotropy by shear-wave splitting: Geophysics, v. 50, p. 142–152, doi:10.1190/1.1441824.

Eken, T., Plomerová, J., Roberts, R., Vecsey, L., Babuška, V., Shomali, H., and Bodvarsson, R., 2010, Seismic anisotropy of the mantle lithosphere beneath the Swedish National Seismological Network (SNSN): Tectonophysics, v. 480, p. 241–258, doi:10.1016/j.tecto.2009.10.012.

Feng, M., Assumpção, M., and Van der Lee, S., 2004, Group-velocity tomography and lithospheric S-velocity structure of the South American continent: Physics of the Earth and Planetary Interiors, v. 147, no. 4, p. 315–331, doi:10.1016/j.pepi.2004.07.008.

Feng, M., Van der Lee, S., and Assumpção, M., 2007, Upper mantle structure of South America from joint inversion of waveforms and fundamental-mode group velocities of Rayleigh waves: Journal of Geophysical Research, v. 112, B04312, doi:10.1029/2006JB004449.

Fouch, M.J., and Rondenay, S., 2006, Seismic anisotropy beneath stable continental interiors: Physics of the Earth and Planetary Interiors, v. 158, p. 292–320, doi:10.1016/j.pepi.2006.03.024.

Fouch, M.J., Fischer, K.M., Parmentier, E.M., Wysession, M.E., and Clarke, T.J., 2000, Shear wave splitting, continental keels, and patterns of mantle flow: Journal of Geophysical Research, v. 105, p. 6255–6275.

Gripp, A.E., and Gordon, R.G., 2002, Young tracks of hotspots and current plate velocities: Geophysical Journal International, v. 150, p. 321–361, doi:10.1046/j.1365-246X.2002.01627.x.

Growdon, M.A., Pavlis, G.L., Niu, F., Vernon, F.L., and Rendon, H., 2009, Constraints on mantle flow at the Caribbean–South American plate boundary inferred from shear wave splitting: Journal of Geophysical Research, v. 114, B02303, doi:10.1029/2008JB005887.

Gung, Y., Panning, M., and Romanowicz, B., 2003, Global anisotropy and the thickness of continents: Nature, v. 422, p. 707–711, doi:10.1038/nature01559.

Heintz, M., Vauchez, A., Assumpção, M., Barruol, G., and Egydio-Silva, M., 2003, Shear wave splitting in SE Brazil: An effect of active or fossil upper mantle flow, or both: Earth and Planetary Science Letters, v. 211, p. 79–95, doi:10.1016/S0012-821X(03)00163-8.

Heit, B., Sodoudi, F., Yuan, X., Bianchi, M., and Kind, R., 2007, An S receiver function analysis of the lithospheric structure in South America: Geophysical Research Letters, v. 34, L14307, doi:10.1029/2007GL030317.

Helffrich, G., Wiens, D.A., Vera, E., Barrientos, S., Shore, P., Stacey, R., and Adaros, R., 2002, A teleseismic shear-wave splitting study to investigate mantle flow around South America and implications for plate-driving forces: Geophysical Journal International, v. 149, p. F1–F7, doi:10.1046/j.1365-246X.2002.01636.x.

Ivan, M., Silva, L.J.H., and Marza, V., 2001, Probing the subcontinental South American upper mantle with SKS splitting at some selected Brazilian stations: Revue Roumaine de Géophysique, v. 45, p. 39–57.

James, D.E., and Assumpção, M., 1996, Tectonic implications of S-wave anisotropy beneath SE Brazil: Geophysical Journal International, v. 126, p. 1–10, doi:10.1111/j.1365-246X.1996.tb05263.x.

Julià, J., Assumpção, M., and Rocha, M., 2008, Deep crustal structure of the Paraná Basin from receiver functions and Rayleigh-wave dispersion: Evidence for a fragmented cratonic root: Journal of Geophysical Research, v. 113, B08318, doi:10.1029/2007JB005374.

Kendall, J.M., and Silver, P.G., 1998, Investigating causes of D″ anisotropy, *in* Gurnis, M., Wysession, M., Knittle, E., and Buffet, B., eds., Core-Mantle Boundary Region: American Geophysical Union Geodynamic Monograph 28, p. 97–118.

Krüger, F., Scherbaum, F., Rosa, J.W.C., Kind, R., Zetsche, F., and Höhne, J., 2002, Crustal and upper mantle structure in the Amazon region (Brazil) determined with broadband mobile stations: Journal of Geophysical Research, v. 107, no. B10, p. 2265, doi:10.1029/2001JB000598.

Lloyd, S., van der Lee, S., França, G.S., Assumpção, M., and Feng, M., 2010, Moho map of South America from receiver functions and surface waves: Journal of Geophysical Research, v. 115, B11315, doi:10.1029/2009JB006829.

Masy, J., Niu, F., and Levander, A., 2009, Seismic anisotropy and mantle flow beneath western Venezuela [abs]: American Geophysical Union Fall Meeting 2009, paper T53A-1554.

Nicolas, A., and Christensen, N.I., 1987, Formation of anisotropy in upper mantle peridotites—A review, *in* Fuchs, K., and Froidevaux, C., eds., Composition, Structure and Dynamics of the Lithosphere-Asthenosphere System: Washington, D.C., American Geophysical Union, p. 111–123.

Piñero-Feliciangeli, L.T., and Kendall, J.-M., 2008, Sub-slab mantle flow parallel to the Caribbean plate boundaries: Inferences from SKS splitting: Tectonophysics, v. 462, p. 22–34, doi:10.1016/j.tecto.2008.01.022.

Plomerová, J., Frederiksen, A.W., and Park, J., 2008, Seismic anisotropy and geodynamics of the lithosphere-asthenosphere system: Tectonophysics, v. 462, p. 1–6, doi:10.1016/j.tecto.2008.08.007.

Polet, J., Silver, P.G., Beck, S., Wallace, T., Zandt, G., Ruppert, S., Kind, R., and Rudloff, A., 2000, Shear wave anisotropy beneath the Andes from the BANJO, SEDA, and PISCO experiments: Journal of Geophysical Research, v. 105, no. B3, p. 6287–6304, doi:10.1029/1999JB900326.

Ritsema, J., van Heijst, H.J., and Woodhouse, J.H., 2004, Global transition zone tomography: Journal of Geophysical Research, v. 109, B02302, doi:10.1029/2003JB002610.

Rocha, M.P., Schimmel, M., and Assumpção, M., 2011, Upper-mantle seismic structure beneath SE and Central Brazil from P- and S-wave regional traveltime tomography: Geophysical Journal International, v. 184, p. 268–286, doi:10.1111/j.1365-246X.2010.04831.x.

Russo, R.M., and Silver, P.G., 1994, Trench-parallel flow beneath the Nazca plate from seismic anisotropy: Science, v. 263, p. 1105–1111, doi:10.1126/science.263.5150.1105.

Savage, M.K., 1999, Seismic anisotropy and mantle deformation: What have we learned from shear wave splitting?: Reviews of Geophysics, v. 37, no. 1, p. 65–106, doi:10.1029/98RG02075.

Schimmel, M., Assumpção, M., and VanDecar, J.C., 2003, Seismic velocity anomalies beneath SE Brazil from P and S wave travel time inversions: Journal of Geophysical Research, v. 108, no. B4, doi:10.1029/2001JB000187.

Schobbenhaus, C., and Bellizzia, A., coordinators, 2000, Geological Map of South America: Brasília, Brazil, CPRM (Brazilian Geological Survey), scale 1:5,000,000.

Silver, P.G., 1996, Seismic anisotropy beneath the continents: Probing the depths of geology: Annual Review of Earth and Planetary Sciences, v. 24, p. 385–432, doi:10.1146/annurev.earth.24.1.385.

Silver, P.G., and Chan, W.W., 1991, Shear wave splitting and subcontinental mantle deformation: Journal of Geophysical Research, v. 96, no. 10, p. 16,429–16,454, doi:10.1029/91JB00899.

Tassinari, C.C.G., and Macambira, M.J.B., 1999, Geochronological provinces of the Amazonian craton: Episodes, v. 22, no. 3, p. 174–182.

Tommasi, A., 1998, Forward modeling of the development of seismic anisotropy in the upper mantle: Earth and Planetary Science Letters, v. 160, p. 1–13, doi:10.1016/S0012-821X(98)00081-8.

Tommasi, A., Mainprice, D., Cordier, P., Thoraval, C., and Couvy, H., 2004, Strain-induced seismic anisotropy of wadsleyite polycrystals and flow patterns in the mantle transition zone: Journal of Geophysical Research, v. 109, B12405, doi:10.1029/2004JB003158.

Trampert, J., and van Heijst, H.J., 2002, Global azimuthal anisotropy in the transition zone: Science, v. 296, no. 5571, p. 1297–1299, doi:10.1126/science.1070264.

Vauchez, A., and Nicolas, A., 1991, Mountain building: Strike-parallel motion and mantle anisotropy: Tectonophysics, v. 185, p. 183–201, doi:10.1016/0040-1951(91)90443-V.

Vecsey, L., Plomerová, J., Kozlovskaya, E., and Babuška, V., 2007, Shear wave splitting as a diagnostic of varying anisotropic structure of the upper mantle beneath central Fennoscandia: Tectonophysics, v. 438, p. 57–77, doi:10.1016/j.tecto.2007.02.017.

Vinnik, L.P., Makeyeva, L.I., Milev, A., and Usenko, A.Y., 1992, Global patterns of azimuthal anisotropy and deformation in the continental mantle: Geophysical Journal International, v. 111, p. 433–447, doi:10.1111/j.1365-246X.1992.tb02102.x.

Wang, X., Ni, J.F., Aster, R., Sandvol, E., Wilson, D., Sine, C., Grand, S.P., and Baldridge, S., 2008, Shear-wave splitting and mantle flow beneath the Colorado Plateau and its boundary with the Great Basin: Bulletin of the Seismological Society of America, v. 98, no. 5, p. 2526–2532, doi:10.1785/0120080107.

Wolfe, C., and Silver, P.G., 1998, Seismic anisotropy of oceanic upper mantle: Shear wave splitting methodologies and observations: Journal of Geophysical Research, v. 103, p. 749–771, doi:10.1029/97JB02023.

Wookey, J., Kendall, J.M., and Barruol, G., 2002, Mid-mantle deformation inferred from seismic anisotropy: Nature, v. 415, no. 6873, p. 777–780.

Wüstefeld, A., Bokelmann, G., Zaroli, C., and Barruol, G., 2008, SplitLab: A shear-wave splitting environment in Matlab: Computers & Geoscience, v. 34, p. 515–528, doi:10.1016/j.cageo.2007.08.002.

MANUSCRIPT RECEIVED 1 FEBRUARY 2010
REVISED MANUSCRIPT RECEIVED 21 DECEMBER 2010
MANUSCRIPT ACCEPTED 26 DECEMBER 2010

Printed in the USA